J Mater Sci: Mater Med (2009) 20:1945–1953
DOI 10.1007/s10856-009-3741-1

Immobilization of lactobionic acid on the surface of cadmium sulfide nanoparticles and their interaction with hepatocytes

K. M. Kamruzzaman Selim · Zhi-Cai Xing · Haiqing Guo · Inn-Kyu Kang

Received: 14 April 2008 / Accepted: 23 March 2009 / Published online: 14 April 2009

Abstract In the current study, β-galactose-carrying lactobionic acid (LA) was conjugated on the surface of mercaptoacetic acid-coated cadmium sulfide nanoparticles (CSNPs) to ensure specific recognition of liver cells (hepatocytes) and to enhance biocompatibility. Maltotrionic acid-coated CSNPs (MCSNPs) were also prepared for use as a control. The results showed that LA-immobilized CSNPs (LCSNPs) were selectively and rapidly internalized into hepatocytes and emitted more intense fluorescence images as well as demonstrated increased biocompatible behavior in vitro than those of CSNPs and MCSNPs. Furthermore, the uptake amount of LCSNPs into hepatocytes was higher than that of CSNPs and MCSNPs. All these results indicate that LCSNPs may find ever-growing applications in biological labels and detection or contrast agents in life science and medical diagnostics.

1 Introduction

Quantum dots (Q-dots), nanometer-scale semiconductor crystals, have attracted widespread attention in various fields of biology and medicine as a new class of molecular imaging agents [1, 2]. Compared with traditional organic dyes and fluorescent proteins, Q-dots (CdS, CdSe ZnS, CdTe etc.) are considered to be ideal candidates as fluorescent probes for long-term imaging to track whole cells or intracellular biomolecules. This is due to their several unique advantages, such as higher levels of brightness (10–20 times brighter than organic dyes), narrow emission, broad excitation and higher photostability [3, 4].

Despite the increasing popularity of Q-dots as cell labeling agents, their cytotoxicity remains a major concern [5]. Q-dots contain toxic components such as cadmium (from cadmium chalcogenide-based Q-dots) or lead (from lead chalcogenide-based Q-dots). Cd^{+2} and Pb^{+2} could be released from Q-dots and then kill the cells [6, 7]. So, depending on the applications, surface modifications of Q-dots are required. For example, biomedical applications require high-quality water soluble and non-toxic Q-dots. The surfaces of Q-dots are coated with soluble ligands for making Q-dots water soluble and suitable for use in cell biology [8]. The coating materials can be low or nontoxic organic molecules/polymers or inorganic layers [6]. So far, numerous modifications of the Q-dots surface chemistry have been explored, including the attachment of organic layers of poly(ethylene glycol) (PEG) [9, 10], mercaptoacetic acid [11, 12], mercaptopropionic acid [13], mercaptobenzoic acid [14] and biocompatible and chemically functionalizable inorganic shells such as silica or zinc sulfide [9, 15]. All these coatings can mainly ensure the water solubility of Q-dots and are unable to enhance the biocompatibility considerably. In fact, these coatings alone are insufficient to stabilize the core of Q-dots, particularly in biological solutions [16]. Therefore, further coating with suitable water-soluble organic ligand/biomolecules is necessary to enhance the biocompatibility of Q-dots considerably. The biomolecules attachment on a Q-dots surface is essential not only for

K. M. Kamruzzaman Selim · Z.-C. Xing · I.-K. Kang (✉)
Department of Polymer Science, Kyungpook National University, Daegu 702-701, South Korea
e-mail: ikkang@knu.ac.kr

H. Guo
School of Molecular Engineering and Chemistry, Peking University, Beijing, China

enhancing biocompatibility, but also for introducing specific functionalities. From another perspective, it may be stated that biological molecules can be fluorescence labeled by attaching Q-dots. Biofunctionalization has been achieved so far by conjugation or complexation of Q-dots with targeting moieties to facilitate the uptake of nanoparticles [17]. To that end, so far Q-dots have been covalently linked with biorecognition molecules such as: biotin [18], folic acid [3], neurotransmitter serotonin [19], peptides [12, 20], proteins like avidin or streptavidin [21], bovine serum albumin [22], transferrin [11], antibodies [23] and DNA [24]. But, to the best of our knowledge, no report has yet been published using β-galactose carrying lactobionic acid (LA) as a coating material of Q-dots to ensure specific recognition of cells (hepatocytes) and facilitate the uptake into cells while reducing the toxicity of Q-dots. β-galactose carrying lactobionic acid was chosen because it is known as a specific adhesive ligand to asialoglycoprotein (AGP) receptors of liver cells (hepatocytes) and its biocompatibility has already been proven [25–27]. Therefore, it is one of the strongest candidates to serve all three purposes (ensuring specific targeting, facilitating uptake into cells and enhancing biocompatibility of Q-dots).

In the current study, mercaptoacetic acid-coated cadmium sulfide nanoparticles (CSNPs), typical semiconductor Q-dots, were synthesized in an aqueous medium by the arrested precipitation method at room temperature. Then, lactobionic acid (LA) was immobilized on the surface of the CSNPs (LCSNPs) as a targeting moiety to ensure specific recognition of the liver cells (hepatocytes), to facilitate the uptake of nanoparticles into cells and to enhance the biocompatibility. Maltotrionic acid (MA)-coated CSNPs (MCSNPs) were also prepared as a control. The surface properties of CSNPs, MCSNPs and LCSNPs were characterized by various physicochemical means and then, fluorescent microscopy was used to visualize the uptake and track the distribution of the nanoparticles into hepatocytes. Finally, the uptake amount of CSNPs, MCSNPs and LCSNPs into cells (hepatocytes) was measured using Inductively Couple Mass Spectroscopy (ICP-Mass).

2 Experimental section

2.1 Materials

Cadmium chloride ($CdCl_2$ 2.5 H_2O >98%), Sodium sulfide (Na_2S $9H_2O$, 98.0%) and mercaptoacetic acid (HS-CH_2COOH) were purcheased from Sigma-Aldrich Co. (USA). Ethylenediamine was purcheased from Duksan Pharmaceuticals Co. Ltd (Korea). Lactobionic acid, maltotriose and Amberlite IR-120 ion exchange resin were purchased from Aldrich Chemical Co. (USA) while 3-(4,5-dimethylazol-2-yl)-2,5-diphenyl-2H-tetrazolium bromide (MTT) was purchased from Sigma Co. All other chemicals used in this study were analytical grade and used without further purification.

2.2 Synthesis of water soluble CSNPs

Water soluble CSNPs were synthesized using the previously published method [12]. Briefly, carboxyl-stabilized CSNPs were synthesized by arrested precipitation at room temperature in an aqueous solution using mercaptoacetic acid as the colloidal stabilizer. Nanocrystals were prepared from a stirred solution of 0.0456 g $CdCl_2$ (5 mM) in 40 ml of pure water. The pH was lowered to 2 with mercaptoacetic acid and then raised to 7 with concentrated NaOH. The mixture was deaerated by N_2 bubbling for about 30 min and then, a freshly prepared 40 ml of 5 mM Na_2S (0.0480 g Na_2S in 40 ml water) was added to the mixture with rapid stirring. The solution turned yellow shortly after the sulfide addition due to the cadmium sulfide nanoparticles formation (CSNPs) (reaction scheme is shown in Fig. 1a). CSNPs were separated from reaction byproducts by precipitation with the addition of acetone (4 ml of acetone/ml of nanocrystal solution). The precipitate was isolated by centrifugation and dried in a freeze dryer. The powder CSNPs are redispersible in water, whereby a clear colloidal solution can be obtained. The free carboxylic acid groups of the prepared CSNPs are suitable for covalent coupling to various biomolecules by covalent interaction to reactive amine groups.

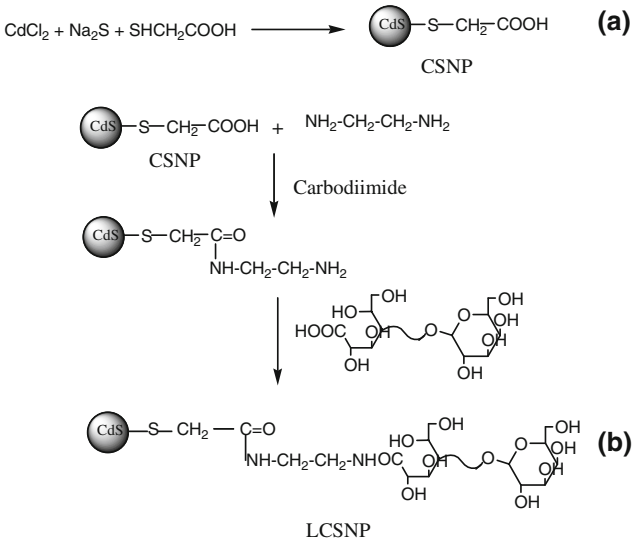

Fig. 1 Schematic diagram showing the synthesis of **a** CSNPs and **b** LCSNPs

2.3 Conjugation of CSNPs with LA

Conjugation of CSNPs with LA involved two steps. First, CSNPs were reacted with ethylenediamine to introduce amine groups on the surfaces. To do so, CSNPs (0.5 g) were dissolved in an aqueous solution (20 ml) containing 1-ethyl-3-(3-dimethylaminopropyl)-carbodiimide hydrochloride (EDC, 4 mg/ml) and stirred for 4 h to activate the carboxylic acid groups on the surface. Then, the excess amount of ethylenediamine was added to the solution and stirred for 24 h to obtain amine-grafted CSNPs. To keep free amine groups at one end of the ethylenediamine after the reaction, an excessive amount of ethylenediamine was used in the coupling reaction with the carboxylic acid groups on the surface [28]. The amine-conjugated CSNPs were isolated via repeated centrifugation and finally dried in a freeze dryer. In the second step, LA was immobilized on the surfaces of amine-conjugated CSNPs as follows: LA (1.8 g, 0.005 mmol) was dissolved in a 0.75 N sodium citrate buffer solution (25 ml, pH 4.7) containing 1-ethyl-3-(3-dimethylaminopropyl) carbodiimide hydrochloride (EDC) and incubated at 4°C for 5 h to activate the carboxylic acid groups of LA. Then, primary amine-coated CSNPs (0.5 g) were added to this solution and the mixture was stirred for 48 h at room temperature to obtain LA-coated CSNPs (LCSNPs) as shown in Fig. 1b. LCSNPs were isolated by repeated centrifugation and stored in phosphate buffered saline (PBS) at pH 7. All the conjugation reactions, unless otherwise noted, were carried out in the dark under a N_2 ambient environment. For use as control, maltotrionic acid (MA)-coated CSNPs (MCSNPs) were also prepared. MA is not commercially available. MA was prepared from maltotriose following the procedure reported by K. M. K. Selim et al. [29]. MA was then conjugated with amine-coated CSNPs. The conjugation procedure was the same as was mentioned in the case of LA.

2.4 Surface characterization

Fourier transform infrared (FT-IR) spectra were obtained using a Jasco, FT-IR 300E spectrometer with a resolution of 4 cm^{-1}. Dried samples were ground with KBr powder and compressed into pellets for FT-IR examination. Transmission electron microphotographs (PHILIPS, CM 200 TEM, applied operation voltage; 120 kV) were used to observe the morphology of nanoparticles. To obtain the samples for TEM observations, particles were diluted with distilled water and then deposited on Formvar-coated 400 mesh copper grids. After drying the nanoparticles' fluids thin films on the copper grid, a thin layer of carbon films of about 10–30 nm in thickness was deposited on the nanoparticles fluids film. The hydrodynamic diameter and size distribution were determined by dynamic light scattering (DLS) by means of a standard laboratory-built light scattering spectrometer using a BI 90 particle sizer (Brookhaven Instruments Corp., Holtsville, NY). It had a vertically polarized incident light of 514.5 nm supplied by an argon ion laser (Lexel laser, model 95). The UV-vis absorption spectrum was recorded from aqueous dispersions at room temperature using a Hitachi U-3000 Spectrophotometer. To investigate the crystal structure of CSNPs, X-ray diffraction (XRD, Enraf Nonius, RA/FR-571) was used. The result was compared with JCPDS file no. 10-454 to confirm whether any impurity phase exists in CSNPs.

2.5 Cell culture experiment

2.5.1 Hepatocyte isolation and culture

Primary hepatocytes were isolated from a SD rat (5–7 weeks old, male, Daehan Biolink Co., Korea) using the modified in situ perfusion method [26]. The dead hepatocytes were removed by density gradient centrifugation on Percoll (Amersham Pharmacia Biotech, Sweden). The Percoll solution (1.065 g/ml) used for the recovery of hepatocytes was prepared by diluting Percoll (1.13 g/ml) with Hank's solution. The viable primary hepatocytes were suspended in a William's E medium containing penicillin (50 mg/ml) and HEPES (10 mM). Only the isolated hepatocytes with greater than 90% viability by trypan blue dye exclusion were used for the experiments. The cell density was adjusted to 1×10^5 cell/ml in a William's E medium containing 200 U/ml of penicillin and 200 mg/ml streptomycin.

2.5.2 In vitro cytotoxicity

To assess the cytotoxicity of CSNPs, MCSNPs, LCSNPs, the viability of hepatocytes was measured by (3-{4,5-dimethylthiazol-2yl}-2,5-diphenyl-2H-tetrazolium bromide) (MTT) assay. The untreated hepatocytes were used as control. The mechanism behind this assay is that the reduction of the tetrazolium salt into a blue color product (formazan) only occurs in metabolically active cells. The amount of formazan produced is proportional to the number of living cell [30]. Briefly, hepatocytes were seeded (1×10^5 cell/ml) on 24 well plates in the presence of a cell culture medium. After 24 h, the culture medium was replaced with a fresh medium containing CSNPs, MCSNPs and LCSNPs at a particle concentration of 0.2 mg/ml. After being incubated for 1, 2, 3, 4, 5 days, a 50 µl MTT solution (5 mg/ml in PBS) was added to each well and incubated in a humidified atmosphere of 5% CO_2 at 37°C for 4 h. After removing the medium, the converted dye was

dissolved in acidic isopropanol (0.04 N HCl-isopropanol) and kept for 30 min in the dark at room temperature. From each sample, the medium (100 µl) was taken and transferred to a 96-well plate and subjected to ultraviolet measurements for converted dye. This was done at a wavelength of 570 nm on a kinetic microplate reader (EL × 800, Bio-T® Instruments, Inc, Highland Park, USA). The experiment was repeated three times. Cell viability of untreated hepatocytes (control) at the first day of incubation was considered 100% and viability was expressed as a percentage of control. In order to obtain complementary evidence, the biochemical assay of viability was confirmed by optical microscope (Nikon Eclipse TS100, Japan). To do so, cells were seeded at the density of 1×10^5 cell/ml. Then, CSNPs, LCSNPs and MCSNPs at the concentration of 0.2 mg/ml were added to the cell solution and maintained at 37°C in a humidified air/CO_2 incubator (95/5 vol%) with incubation time of 96 h and the morphology of adhered cells was observed.

2.5.3 *In vitro imaging*

Hepatocytes were seeded at a concentration of 1×10^5/ml in a 10 ml petridish and incubated for 1 day. After 1 day the medium was replaced with CSNPs, MCSNPs and LCSNPs containing media at a particle concentration of 0.2 mg/ml and incubated further at different times such as 30 min, 1 h, 2 h, 3 h and 4 h to find the minimum time required for the internalization of the nanoparticles into cells. Then, the cells were washed three times with Dulbecco's PBS (D-PBS) and observed with a laser scanning fluorescence microscopy. Fluorescence images were obtained using an Olympus IX70 fluorescence microscope equipped with a cooled charge-coupled device (CCD) camera. Capturing and processing images were done by using DVC view software (version 2.2.8, DVC Company).

2.5.4 *Cellular uptake*

To quantify the intracellular uptake of the nanoparticles, cells were grown in 24-well culture plates, with approximately 10^5 cells in 1 ml of medium. After incubation at 37°C for 20 h, the cells were reseeded using culture medium containing nanoparticles at a concentration of 0.2 mg/ml. In control cultures, the cells were placed in 1 ml medium without nanoparticles at the same cell density. The intracellular cadmium concentration was quantified using ICP mass spectroscopy. Cells were washed with D-PBS, detached using trypsin-EDTA, resuspended in 10 ml of culture media, counted, centrifuged down, and the cell pellet was dissolved in 37% HCl solution at 70°C for 30 min. The samples were diluted to a final cadmium concentration of 1.0 – 4.0 mg/ml. The experiment was carried out three times and the results were averaged with standard deviation.

2.5.5 *Statistical analysis*

The cell viability experiments were performed in triplicate and the results were expressed as mean ± standard deviation (SD). The student's t test was employed to assess statistical significant difference of the results. Difference was considered statistically significant at $P < 0.05$.

3 Results and discussion

3.1 Surface characterization

The X-ray diffraction spectrum of CSNPs is shown in Fig. 2. It was compared with the data of the JCPDS file no. 10–454 and is in good agreement with that of pure cubic-phase cadmium sulfide, without signals from $CdCl_2$, NaOH and other precursor compounds. The three peaks observed in Fig. 2 at 2θ values of 26.439°, 43.862° and 51.389° correspond to the three crystal planes of (111), (220) and (311), indicating that the CSNPs are in a cubic phase [31]. Again, the diffraction peaks of the CSNPs are somewhat broadened. The broadness of the peaks indicates that the dimensions of the CSNPs were very small. The synthesis of cadmium sulfide was further confirmed by an UV-vis absorption spectrum as shown in Fig. 3. The CSNPs sample showed an absorption onset at 410 nm and exhibited a blue shift compared to 512 nm for bulk cadmium sulfide [32]. This blue shift was caused by strong quantum confinement, due to the decrease in particle size [33].

The surface modification of CSNPs with LA and MA was confirmed by FT-IR, as displayed in Fig. 4 together with the FT-IR spectrum of CSNPs and amine-coated CSNPs. For

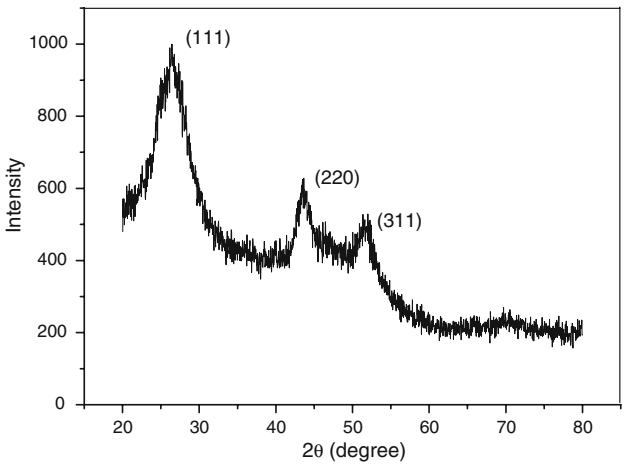

Fig. 2 XRD pattern of CSNPs

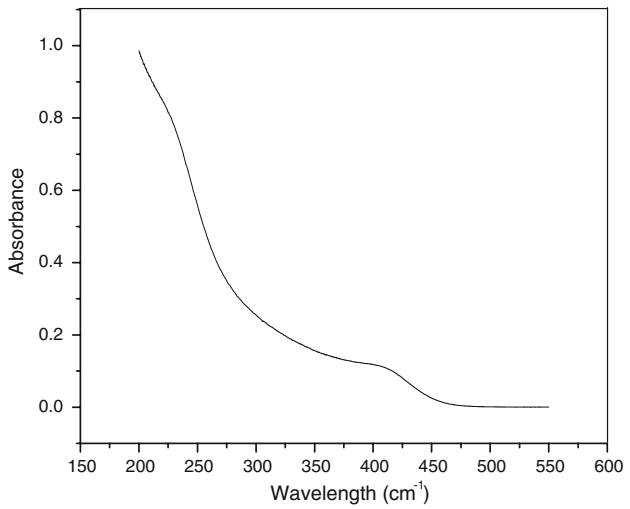

Fig. 3 UV-vis spectrum of CSNPs

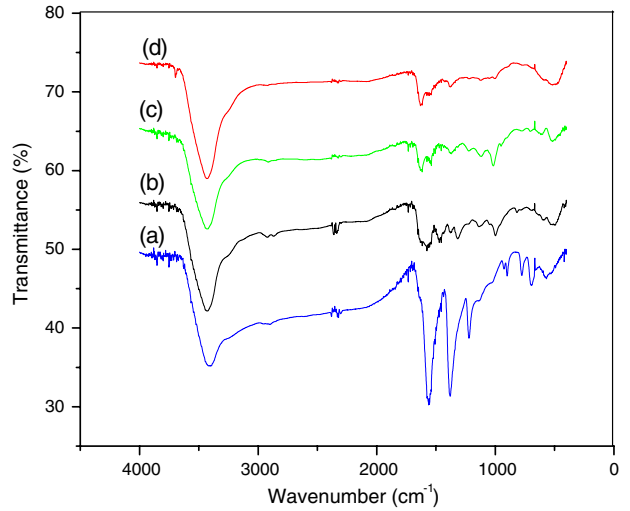

Fig. 4 FTIR spectra of **a** CSNPs, **b** amine-coated CSNPs, **c** LCSNPs and **d** MCSNPs

CSNPs (Fig. 4a), two distinctive bands were observed at 1559 cm^{-1} and 1375 cm^{-1}. This is due to C–O antisymmetric stretching and C–O symmetric stretching bands of acetate ion (COO–), respectively which clearly indicate the formation of co-ordinate bond between the oxygen atom of mercaptoacetic acid and Cd^{+2}. No free carboxyl acid band at 1800–1740 cm^{-1} due to the C=O stretching band is observed in the capped nanoparticles [34]. The introduction of amine groups on the surface of CSNPs was confirmed by the characteristic peak at 1570 cm^{-1} as shown in Fig. 4b, which attributed to free amine ($–NH_2$) groups. Again, LA and MA are found to exhibit characteristic peaks at 3450 cm^{-1} and 1740 cm^{-1} which correspond to hydroxyl (–OH) and carboxyl (–COOH) groups, respectively [25, 29]. Though peaks at 3450 cm^{-1} were observed, no peak at position 1740 cm^{-1} was found in the spectrum of LCSNPs (Fig. 4c) and MCSNPs (Fig. 4d). Instead peaks at positions around 1632 cm^{-1} and 1552 cm^{-1} were observed in both the spectrum of LCSNPs (Fig. 4c) and MCSNPs (Fig. 4d), which are assined to –CO–NH–(amide I) and –CO–NH–(amide II) bonds, respectively. This is because, after the reaction of free amine groups of amine-coated CSNPs with LA and MA, the absorption at 1740 cm^{-1} based on carboxylic acid disappeared, but the absorption at 1632 cm^{-1} and 1552 cm^{-1} appeared based on an amide bond between the carboxylic acid of LA and MA and the surface amine groups of ethylenediamine-coated CSNPs. The –CO–NH mode contains contributions from C–N stretching vibration and N–H bending vibration which originate from the bonding between carboxylic groups of CSNPs (Fig. 4a) and the amine groups of the ethylenediamine chain. These phenomena indicate that LA and MA were successfully immobilized on the surface of CSNPs.

The TEM images of CSNPs and LCSNPs are shown in Fig. 5a and b, respectively. It was observed that CSNPs have a spherical morphology with an average diameter of ca. 4.5 nm. Because of the small dimensions and high surface energy of the particles, it is easy for them to aggregate as seen in Fig. 5a. On the other hand, the particles are shaped spherically and monodispersed with an average size of ca. 10 nm in the case of LCSNPs (Fig. 5b). It was also found from this figure that the morphology of the particles is almost homogeneous. This monodispersity and larger particles size phenomena may have happened due to the attachment of LA on the surface of CSNPs.

Figure 6 shows the typical size and size distribution of synthesized CSNPs (Fig. 6a) and LCSNPs (Fig. 6b) measured by DLS. It can be observed from Fig. 6a that the size distribution of CSNPs is a bimodal size distribution: two dominant peaks at around 18 nm whereas there are two minor peaks at around 22 nm. On the other hand, the LCSNPs display a unimodal size distribution (Fig. 6b) and the average hydrodynamic diameter of the LCSNP was about 35 nm. The size as determined by DLS was considerably larger than that determined by TEM. This is because the DLS technique gives a mean hydrodynamic diameter of the CSNPs core surrounded by the organic and solvation layers, and this hydrodynamic diameter is influenced by the viscosity and concentration of the solution [35]. On the other hand, TEM gives the diameter of the core alone. Again, it is clear from Fig. 6a and b that the size distribution of LCSNPs show a narrower and more monodisperse pattern than that of CSNPs.

3.2 Cell cytotoxicity

Cytotoxicity was evaluated by both morphological observations of cells via microscopy and MTT viability assay.

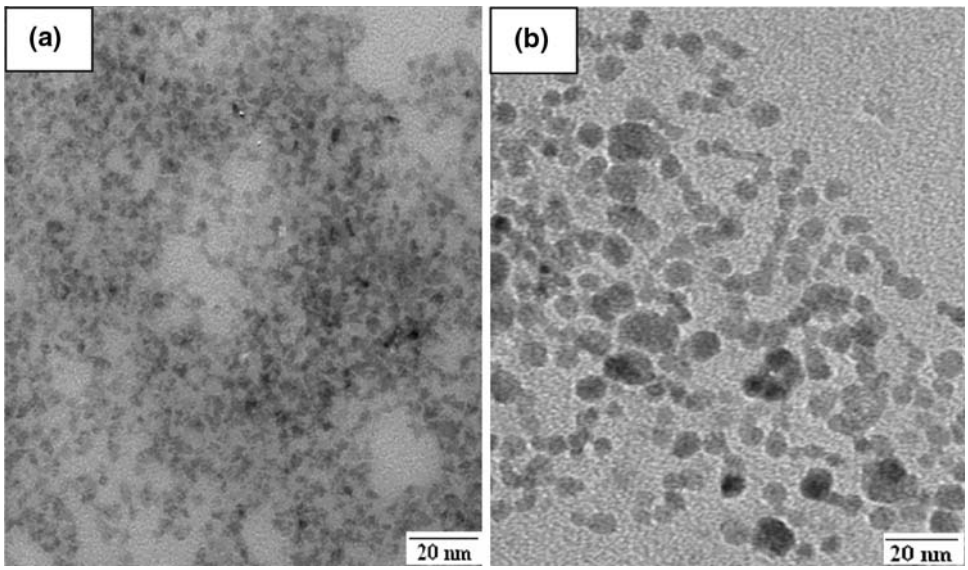

Fig. 5 TEM images of **a** CSNPs and **b** LCSNPs

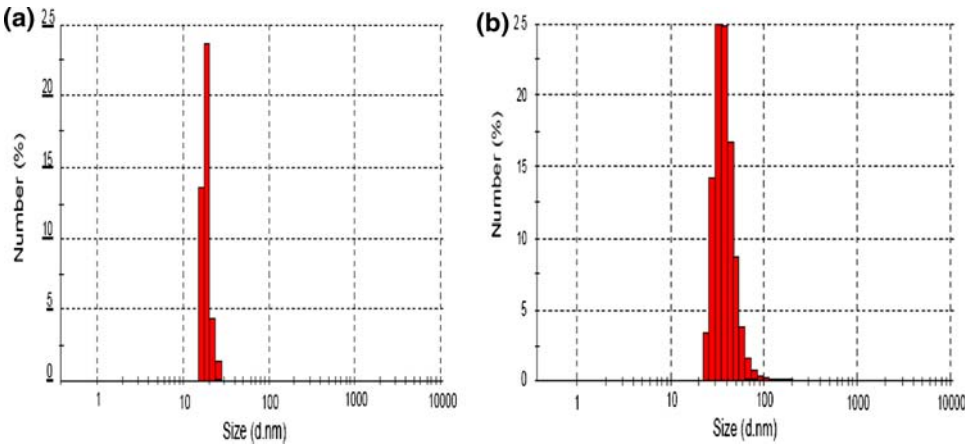

Fig. 6 Particle size distribution of **a** CSNPs and **b** LCSNPs measured by DLS

Figure 7 shows optical microscope photographs of hepatocytes (Fig. 7a), after a 96 h culture in a media containing MCSNPs (Fig. 7b), LCSNPs (Fig. 7c) and CSNPs (Fig. 7d). The morphology of the cells after a 96 h incubation with MCSNPs and LCSNPs were close to that of the control cells (hepatocytes), suggesting good biocompatibility of MCSNPs and LCSNPs over the time frame. On the other hand, the cell morphology of CSNPs as shown in Fig. 7d altered and cell membranes were almost distorted after a 96 h culture. This may be due to the leaking of the interior toxic cadmium ion (Cd^{+2}) from CSNPs into the cell media and causing the cells almost death. Because, mercaptoacetic acid is one of the smallest solubilizing ligands. Therefore, this acid alone is probably unable to prevent surface oxidation in order to make cadmium sulfide nanoparticles well-coated enough to become biological inert. So, this coating fails to bar the diffusion of cadmium for a longer period [36]. On the other hand, LA coating perhaps decreased the surface oxidation and barred the diffusion of Cd^{+2} from the core, resulting the enhanced biocompatibility.

The cytotoxicity of CSNPs, MCSNPs and LCSNPs was also analyzed by MTT assay. The cells (hepatocytes) viability in a media treated with CSNPs, MCSNPs and LCSNPs at days 1, 2, 3, 4, 5 was shown in Fig. 8. Untreated hepatocytes (i.e. hepatocytes without treatment with any type of nanoparticle) were also analyzed as a control and its viability at the first day of incubation was considered as 100%. The results showed that cell viability with CSNPs was lower (around 65%) than that with LCSNPs and MCSNPs (around 80%). A significant decrease in cell viability ($P < 0.05$) was observed after 3 days incubation with CSNPs (Fig. 8d). On the other hand, a non-significant decrease in cell viability was observed up to 4 days when cells were incubated with LCSNPs (Fig. 8b) and MCSNPs (Fig. 8c). However, cell viability with CSNPs, MCSNPs and LCSNPs decreased significantly after 4 days incubation. Therefore, it can be stated that surface coatings can suppress the toxicity for a certain period of time but can not eliminate it forever and how long a Q-dot will be non-toxic depends on the nature of the coating materials [37].

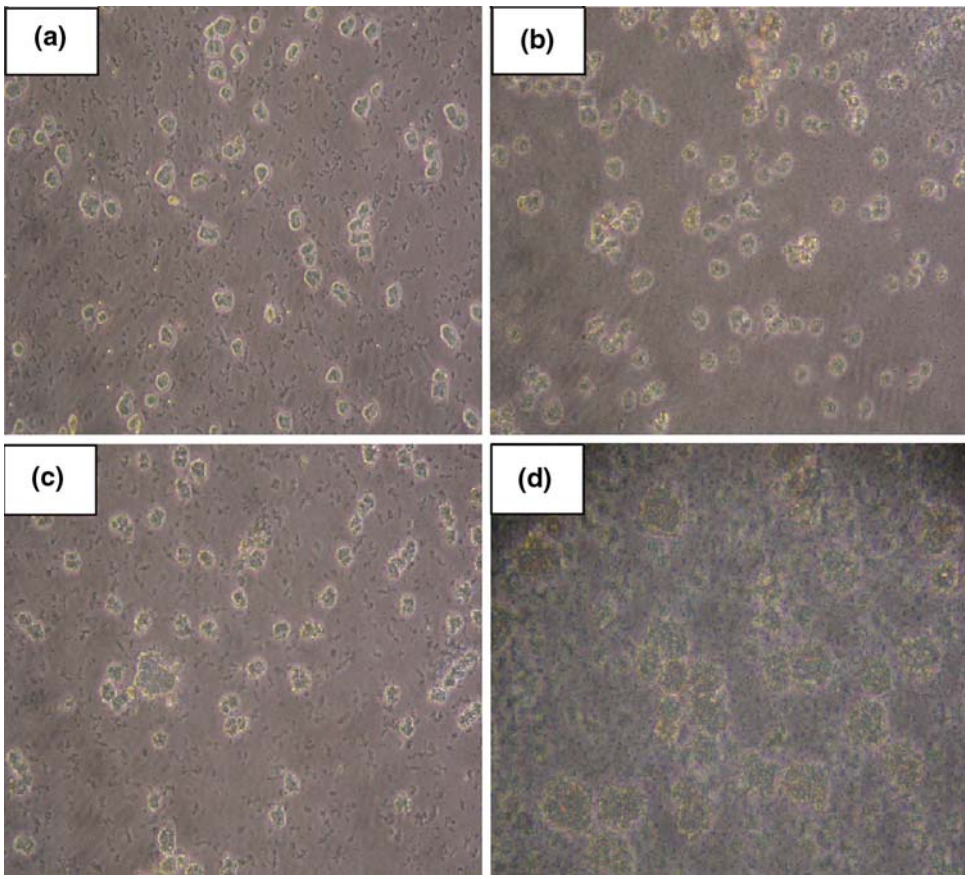

Fig. 7 Optical microscope photographs (×200) of **a** hepatocytes control culture, **b** cells after 96 h of growth in a media containing MCSNPs, **c** LCSNPs and **d** CSNPs

It has been postulated that chalcogenide atoms (Se, S) located on the surface of the Q-dots could be oxidized by oxygen molecules to form oxides (SeO_2, SO_4^{2-}) [38].

$$CdS + 2O_2 \overset{\text{Oxidation}}{\rightarrow} Cd^{2+} + SO_4^{2-}$$

In the case of CSNPs, the formed SO_4^{2-} molecules release from the surface, leaving behind "dangling" reduced Cd atoms. Thus, prolonged exposure of CSNPs to an oxidative environment can cause the decomposition of CSNPs, thereby leading to release of Cd ion into cell media and cause the cells death [36]. On the contrary, in the case of LCSNPs and MCSNPs, surface ligands (LA/MA) decrease surface oxidation of Q-dots by reducing transport of oxygen to the surface. As a result, cell viability with LCSNPs and MCSNP was higher than that with CSNPs over the time range. In other words, it can be mentioned that the surface modification of cadmium sulfide with LA could lessen the cytotoxicity of cadmium sulfide considerably in comparison to that modified by MA and mercaptoacetic acid. Therefore, from the above discussion, it can be stated that cytotoxicity of quantum dots can be kept dormant for a certain period of time (in this study up to 4 days) by polymer coating, but it can not be eliminated forever. It is still a major challenge of using quantum dots in biological system due to their cytotoxicity in nature. But very low dose and polymer coating simultaneously can be a remedy of this problem to some extent [39].

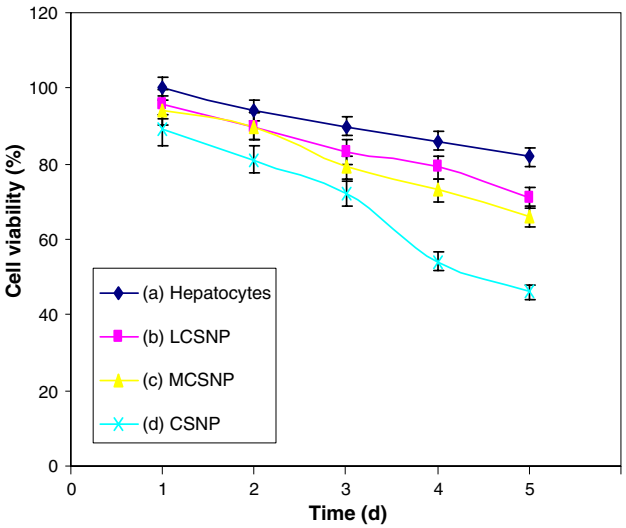

Fig. 8 In vitro viability of hepatocytes **a** untreated hepatocytes, **b** in the presence of LCSNPs, **c** MCSNPs and **d** CSNPs measured by MTT assay. (Data are expressed as mean ± SD ($n = 3$) for the specific absorbance)

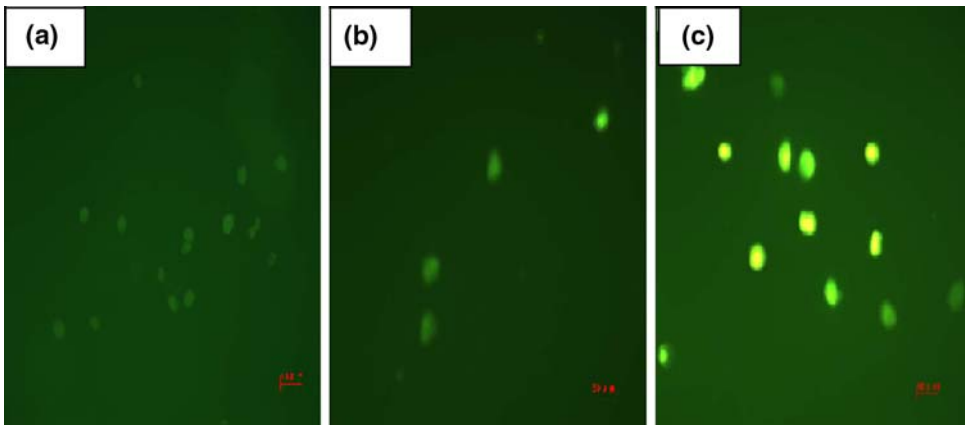

Fig. 9 In vitro fluorescence images of hepatocytes cultured for 3 h in the presence of **a** CSNPs, **b** MCSNPs and **c** LCSNPs

3.3 In vitro cell recognition

Cells (hepatocytes) recognition ability of CSNPs, MCSNPs and LCSNPs was evaluated using fluorescence microscopy. Fluorescence images were investigated after the culture of hepatocytes in the presence of three types of nanoparticles at different time ranges (1, 2, 3 and 4 h). Figure 9 shows fluorescence images obtained from cultured hepatocytes that had been incubated for 3 h with CSNPs (Fig. 9a), MCSNPs (Fig. 9b) and LCSNPs (Fig. 9c). In the absence of LA (Fig. 9a and b), no nanoparticles were observed inside the cells over the time frame and the images resulted from weak cellular autofluorescence. When LA was present (Fig. 9c), nanoparticles were transported into cells (hepatocytes) and emitted fairly intense fluorescence images. This result indicates that galactose moiety carrying LCSNPs provide specific and effective hepatocyte-recognition signals for the nanoparticles to facilitate the internalization into target cells (hepatocytes). The interaction between the LA of LCSNPs and ASG receptor on the membrane surface of the hepatocytes might have contributed to the improvement of the LCSNPs internalization into hepatocytes, based on receptor mediated endocytocis [37]. Similar results were also observed when Chen WCW et al. introduced folic acid [3] and transferring [11] to the surface of Q-dots and consequently interacted with cancer cells.

3.4 Cellular uptake

The uptake of CSNPs, MCSNPs and LCSNPs into hepatocytes was quantified after the cell culture in a media containing 0.2 mg/ml nanoparticles for up to 4 days. Figure 10 shows the uptake of CSNPs (Fig. 10a), MCSNPs (Fig. 10b) and LCSNPs (Fig. 10c) into hepatocytes. The first day's uptake of CSNPs into the cells was 112 pg/cell and the average uptake during the 4 days was 129 pg/cell, i.e., the uptake amount did not increase significantly during the 4 days. Again, the first day's uptake of MCSNPs was 76 pg/cell and the average uptake during the 4 days was

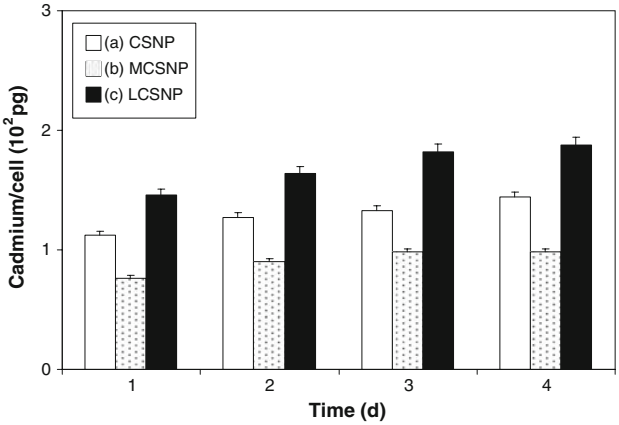

Fig. 10 The amount of **a** CSNPs, **b** MCSNPs and **c** LCSNPs uptaken by hepatocytes at different incubation times

90 pg/cell which was much less than that of CSNPs. But after the modification by LA, the uptake of LCSNPs by hepatocytes increased significantly in comparison to that of CSNPs and MCSNPs and reached 146 pg/cell within the first day of culture. The maximum uptake appeared at 188 pg/cell and the average uptake during the 4 days was 170 pg/cell. This uptake improvement indicates that LA modification not only facilitated the nanoparticles to target specific cells, but also increased the yield of cell internalization. The results also indicate that receptor-mediated endocytosis (in the case of LCSNPs), as well as fluid phase endocytosis (in case of CSNPs and MCSNPs), both happen if longer periods of incubation is allowed.

4 Conclusion

In this study, lactobionic acid (LA) was successfully immobilized on the surface of mercaptoacetic acid-coated cadmium sulfide nanoparticles (CSNPs). The results showed that LA-immobilized CSNPs (LCSNPs) could specifically recognize hepatocytes and emitted intense fluorescence images, as well as demonstrated a higher

efficiency of intracellular uptake into hepatocytes compared to CSNPs and MCSNPs. These results suggest that LCSNPs have a potential to be used in biological applications.

Acknowledgment This work was supported by a grant from the Advanced Medical Technology Cluster for Diagnosis and Prediction at KNU from MOCIE, Republic of Korea.

References

1. Alivisatos AP. Semiconductor clusters, nanocrystals, and quantum dots. Science. 1996;27:933–7.
2. Mitchell P. Turning the spotlight on cellular imaging. Nat Biotechnol. 2001;19:1013–7.
3. Chan WCW, Maxwell DJ, Gao X, Bailey RE, Han M, Nie S. Luminescent quantum dots for multiplexed biological detection and imaging. Curr Opin Biotechnol. 2002;13:40–6.
4. Gao X, Yang L, Petros JA, Marshall FF, Simons JW, Nie S. In vivo molecular and cellular imaging with quantum dots. Curr Opin Biotechnol. 2005;16:63–72.
5. Hsieh SC, Wang FF, Lin CS, Chen YJ, Hung SC, Wang YJ. The inhibition of osteogenesis with human bone marrow mesenchymal stem cells by CdSe/ZnS quantum dot labels. Biomaterials. 2006;27:1656–64.
6. Yu WW, Chang E, Drezek R, Colvin VL. Watersoluble quantum dots for biomedical applications. Biochem Biophy Res Communi. 2006;348:781–6.
7. Celik A, Comelekoglu U, Yalin S. A study on the investigation of cadmium chloride genotoxicity in rat bone marrow using micronucleus test and chromosome aberration analysis. Toxicol Indl Health. 2005;21:243–8.
8. Seydel C. Quantum dots get wet. Science. 2003;300:80–1.
9. Gomez N, Winter JO, Shieh F, Saunders AE, Korgel BA, Schmidt CE. Challenges in quantum dot-neuron active interfacing. Talanta. 2005;67:462–71.
10. Ballou B, Lagerholm BC, Ernst LA, Bruchez MP, Waggoner AS. Noninvasive imaging of quantum dots in mice. Bioconjug Chem. 2004;15:79–86.
11. Chan WCW, Nie S. Quantum dot bioconjugates for ultrasensitive nonisotopic detection. Science. 1998;281:2016.
12. Chen HM, Huang XF, Xu L, Xu J, Chen KJ, Feng D. Self-assembly and photoluminescence of CdS-mercaptoacetic clusters with internal structures. Superlatt Microstruc. 2000;27:1–5.
13. Mitchell GP, Mirkin CA, Letsinger RL. Programmed assembly of DNA functionalized quantum dots. J Am Chem Soc. 1999;121:8122–23.
14. Chen CC, Yet CP, Wang HN, Chao CY. Self-assembly of monolayers of cadmium selenide nanocrystals with dual color emission. Langmuir. 1999;15:6845–50.
15. Chen F, Gerion D. Fluorescent CdSe/ZnS nanocrystal-peptide conjugates for long-term, nontoxic imaging and nuclear targeting in living cells. Nano Lett. 2004;41:1827–32.
16. Jamieson T, Bakhshi R, Petrova D, Pocock R, Imani M, Seifalian AM. Biological applications of quantum dots. Biomaterials. 2007;28:4717–32.
17. Maysinger D, Lovric J, Eisenberg A, Savic R. Fate of micelles and quantum dots in cells. Euro J Pharm Biopharm. 2007;65:270–81.
18. Bruchez M Jr, Moronne M, Gin P, Weiss S, Alivisatos AP. Semiconductor nanocrystals as fluorescent biological labels. Science. 1998;281:2013–6.
19. Rosenthal SJ, Tomlinson I, Adkins EM, Schroeter S, Adams S, Swafford L, et al. Targeting cell surface receptors with ligand-conjugated nanocrystals. J Am Chem Soc. 2002;124:4586–94.
20. Pinaud F, King D, Moore HP, Weiss S. Bioactivation and cell targeting of semiconductor CdSe/ZnS nanocrystals with phytochelatin-related peptides. J Am Chem Soc. 2004;126:6115–23.
21. Jaiswal JK, Mattoussi H, Mauro JM, Simon SM. Long-term multiple color imaging of live cells using quantum dot bioconjugates. Nat Biotechnol. 2003;21:47–51.
22. Hanaki KI, Momo A, Oku T, Komoto A, Maenosono S, Yamaguchi Y, et al. Semiconductor quantum dot/albumin complex is a long-life and highly photostable endosome marker. Biochem Biophys Res Commun. 2003;302:496–501.
23. Goldman ER, Anderson GP, Tran PT, Mattoussi H, Charles PT, Mauro JM. Conjugation of luminescent quantum dots with antibodies using an engineered adaptor protein to provide new reagents for fluoroimmunoassays. Anal Chem. 2002;74:841–7.
24. Gerion D, Parak WJ, Williams SC, Zanchet D, Micheel CM, Alivisatos AP. Sorting fluorescent nanocrystals with DNA. J Am Chem Soc. 2002;124:7070–4.
25. Chung TW, Yang J, Akaike T, Cho KY, Nah JW, Kim SI, et al. Preparation of alginate/galactosylated chitosan scaffold for hepatocyte attachment. Biomaterials. 2002;23:2827–34.
26. Kamruzzaman Selim KM, Ha YS, Kim SJ, Chang Y, Kim TJ, Ho LG, et al. Surface modification of magnetite nanoparticles using lactobionic acid and their interaction with hepatocytes. Biomaterials. 2007;28:710–6.
27. Kang IK, Moon JS, Jeon HM, Meng W, Kim YI, Hwang YJ, et al. Morphology and metabolism of Ba-alginate encapsulated hepatocytes with galactosylated poly(allyl amine) and poly(vinyl alcohol) as extracellular matrices. J Mater Sci: Mater Med. 2005;16:533–9.
28. Bae JS, Seo EJ, Kang IK. Synthesis and characterization of heparinized polyurethanes using plasma glow discharge. Biomaterials. 1999;20:529–37.
29. Selim KMK, Lee JH, Kim SJ, Xing Z, Kang IK, Chang Y, et al. Surface modification of magnetites using maltotrionic acid and folic acid for molecular imaging. Macromol Res. 2006;14:646–53.
30. Chow KS, Khor E, Wan ACA. Porous chitin matrices for tissue engineering: fabrication and in vitro cytotoxic assessment. J Polym Res. 2001;8:27–35.
31. Smith NV. X-ray powder data files American Society for Testing and Materials, Philadelphia; 1967.
32. Pan AL, Ma JG, Yan XZ, Zou BS. The formation of CdS nanocrystals in silica gels by gamma-irradiation and their optical properties. J Phys Condens Matter. 2004;16:3229–38.
33. Brus LE. Electron-electron and electron-hole interactions in small semiconductor crystallites: the size dependence of the lowest excited electronic state. J Chem Phys. 1984;80:4403–9.
34. Kuo YC, Wang Q, Ruengruglikit C, Yu H, Huang Q. Antibody-conjugated CdTe quantum dots for *Escherichia coli* detection. J Phys Chem C. 2008;112:4818–24.
35. Wu YL, Lim CS, Fu S, Tok AIY, Lau HM, Boey FYC, et al. Surface modifications of ZnO qd for bio-imaging. Nanotechnology. 2007;18:1.
36. Derfus AM, Chan WCW, Bhatia SA. Probing the cytotoxicity of semiconductor quantum dots. Nano Lett. 2004;4:11–8.
37. Parak WJ, Pellegrino T, Plank C. Labeling of cells with quantum dot. Nanotechnology. 2005;16:9–25.
38. Spanhel L, Haase M, Weller H, Henglein A. Photochemistry of colloidal semiconductors. 20. Surface modification and stability of strong luminescing CdS particles. J Am Chem Soc. 1987;109:5649–55.
39. Bae PK, Kim KN, Lee SJ, Chang HJ, Lee CK, Park JK. The modification of quantum dot probes used for the targeted imaging of his-tagged fusion proteins. Biomaterials. 2009;30:836–42.